PAPER

Check for updates

Optical sensing of L-dihydroxy-phenylalanine in water by a high-affinity molecular receptor involving cooperative binding of a metal coordination bond and boronate−diol†

María K. Salomón-Flores, [iD] [a] Alejandro O. Viviano-Posadas, [iD] [a] Josue Valdes-García, [iD] [a] Víctor López-Guerrero, [iD] [a] Diego Martínez-Otero, [iD] [a,b] Joaquín Barroso-Flores, [iD] [a,b] Juan M. German-Acacio, [iD] [c] Iván J. Bazany-Rodríguez [iD] [d] and Alejandro Dorazco-González [iD] *[a]

Selective recognition and sensing of catecholamine-based neurotransmitters by fluorescent synthetic receptors capable of operating in pure water is a central topic of modern supramolecular chemistry that impacts biological and analytical chemistry. Despite advances achieved in the recognition of some neuro-transmitters such as dopamine, little effort has been invested in the optical recognition of other neuro-transmitters of paramount importance in biochemistry and medicinal chemistry such as the drug L-dihydroxy-phenylalanine (levodopa). Herein, a cationic Cu(II)−terpyridine complex bearing an intra-molecular fluorescent quinolinium ring covalently linked to phenylboronic acid (**CuL¹**) was synthesized, structurally described by single-crystal X-ray diffraction and studied in-depth as a fluorescent receptor for neurotransmitters in water. The complex **CuL¹** was designed to act as a receptor for levodopa through two Lewis acids of different natures (Cu(II) and B atoms) as cooperative binding points. The receptor **CuL¹** was found to have a strongly acidified −B(OH)₂ group (pK_a = 6.2) and exceptionally high affinity for levo-dopa (K = 4.8 × 10⁶ M⁻¹) with selectivity over other related neurotransmitters such as dopamine, epineph-rine, norepinephrine and nucleosides in the micromolar concentration range at physiological pH. Such levodopa affinity/selectivity for a boronic acid-based receptor in water is still rare. On the basis of spectro-scopic tools (¹¹B NMR, UV-vis, EPR, and fluorescence), high-resolution ESI-MS, crystal structure, and DFT calculations, the interaction mode of **CuL¹** with levodopa is proposed in a 1:1 model using two-point recognition involving a boronate−catechol esterification and a coordination bond Cu(II)−carboxylate. Furthermore, a visual sensing ensemble was constructed using **CuL¹** and the commercial fluorescent dye eosin Y. Levodopa is efficiently detected by the displacement of the eosin Y bound to the Cu(II)−receptor, monitoring its green emission. The use of Cu(II)−boronate complexes for fast and selective neuro-transmitter sensing was unexplored until now.

[a]*Institute of Chemistry, National Autonomous University of Mexico, Ciudad Universitaria, México, 04510 CDMX, Mexico. E-mail: adg@unam.mx*
[b]*Centro Conjunto de Investigación en Química Sustentable, UAEM-UNAM, Instituto de Química, Universidad Nacional Autónoma de México, Carretera Toluca-Atlacomulco Km 14.5, C. P. 50200 Toluca, Estado de México, Mexico*
[c]*Red de Apoyo a la Investigación, Coordinación de la Investigación Científica-UNAM, Instituto Nacional de Ciencias Médicas y Nutrición SZ, Ciudad de México, CP 14000, Mexico*
[d]*Facultad de Química, Universidad Nacional Autónoma de México, Ciudad Universitaria CDMX, 04510 México, Mexico*
†Electronic supplementary information (ESI) available: General information, X-ray crystallographic data, ¹H NMR and ¹³C NMR spectra for ligands **L¹⁻²**, fluori-metric and UV-vis titration experiments and EPR measurements. CCDC 2340947 and 2340948. For ESI and crystallographic data in CIF or other electronic format see DOI: https://doi.org/10.1039/d4dt02108h

Introduction

A central challenge in modern supramolecular chemistry is the selective recognition and optical sensing of catecholamine-based neurotransmitters (NTs) such as dopamine, adrenaline, noradrenaline and levodopa (L-3,4-dihydroxyphenylalanine) in water using synthetic fluorescent receptors.[1–8] These NTs regu-late brain functioning;[9] therefore, selectively sensing and quantifying neurotransmitters provides knowledge about how these biogenic catecholamines drive our motor capacity and physiological functions such as learning, memory, cognition and emotions.[10–12] In general, the physiological concen-trations of these NTs in the cerebrospinal fluid are very low (<10⁻⁶ M), making their selective detection and measurement

difficult.[13] For example, the brain's dopamine concentration ranges from 25 to 40 nM and higher levels are correlated to high blood pressure and cardiotoxicity.[14] In contrast, lower dopamine concentration may cause neurological disorders such as Parkinson's disease, Alzheimer's and schizophrenia.[9,15–17]

Levodopa is a neuromodulator and natural precursor for the biosynthesis of dopamine and epinephrine. It is well known that levodopa can cross the protective blood–brain barrier, unlike the rest of the NTs that cannot pass through it.[18] For this reason, levodopa is a worldwide-prescribed drug for increasing dopamine levels in the brain in the treatment of dopamine-responsive dystonia and Parkinson's disease.[14,19–21] However, recent clinical data have shown that levodopa is toxic when it is in high concentrations.[22] Thus, the levels of levodopa and dopamine in physiological samples are chemical indicators of neurological disorders.[23,24]

To date, an overwhelming majority of levodopa detection methods have been based on electrochemical sensors,[22,25] chromatography,[26] CdSe quantum dots,[8,27–29] TiO_2- nanoparticles,[30] COFs,[31] aptamers[32] and tyrosinase assays.[33] These sensing methods still suffer from some drawbacks such as multiple steps for their construction, particularly for the nanomaterials, as well as long analysis times and the requirement for specialized labs.

Among the different neurotransmitter sensing techniques, fluorescence is particularly desired due to its high sensitivity and real-time response.[4,8,34] Artificial receptors can be exploited as fluorescent chemosensors using various signaling molecular units. While the need for efficient and highly selective optical receptors for levodopa is evident, very few examples have been described to date.

Fluorescent recognition of NTs has been dominated by aldehyde-appended fluorophores able to reversibly react with the amine group from NTs to form imine derivatives, which induce pronounced changes in their optical properties.[5,35–37] However, most of these receptors are not particularly selective, and interference from biological amines such as γ-aminobutyric acid (GABA), histamine, serotonin and amino acids can be a problem. Furthermore, these receptors usually require an organic cosolvent, which seriously limits their applications.[36]

The literature features very few examples of selective receptors for fluorescent sensing of levodopa in water. These receptors include arylboronic acids covalently linked to fluorophores such as metalloporphyrins[38] lucifer yellow,[39] perylene moieties and quinoline rings[40] to yield a conjugated chemosensor. Typically, these borylated receptors show *apparent* binding constants between 10^3 and 10^5 M^{-1} driven by multisite recognition that involves boronate–diol complexation with a catechol skeleton from levodopa and secondary supramolecular interactions (π–π stacking, electrostatic interactions and coordination bonds).[38] They are suitable for sensing levodopa in the micromolar concentration range, but not significantly below, which is highly desirable for sensing levodopa in pharmaceutical and biological samples.[13,34]

On the other hand, fluorescent receptors with a single binding point based on boronic acid have the drawback of not being selective for levodopa.[41,42] Thus, the creation of a fluorescent chemosensor/receptor with high levodopa affinity is not a trivial task and clearly requires elaborate molecular strategy and synthetic approaches to achieve a chemical affinity by both the catechol and carboxylate groups. Previously, Shinkai demonstrated selective two-point binding of levodopa to a boronic-acid-appended Zn(ɪɪ)–porphyrin.[38] In this line, we recently developed molecular receptors for levodopa[43] and fructosyl valine[44] in water that operate by cooperative action of boronic acid and a metal coordination bond. Mainly, Zn(ɪɪ)–terpyridine bearing arylboronic acid complexes exhibited good selectivity and affinity ($K \approx 10^6$ M^{-1}), induced by a complexation boronate–diol and coordination of the carboxylate group from levodopa to a Zn(ɪɪ) atom. Taking into account that Cu(ɪɪ) has a greater carboxylate anion affinity compared to Zn(ɪɪ) and its strong Lewis acidity,[45] we surmised that an efficient levodopa chemosensor could be achieved by using a new water-soluble Cu(ɪɪ)–terpyridine–quinolinium complex bearing a strongly acidified arylboronic acid. The results obtained for a fluorescent Cu(ɪɪ) complex with phenylboronic acid, including synthesis, crystal structure, spectroscopic neurotransmitter sensing studies and theoretical DFT calculations, are summarized below.

Results and discussion
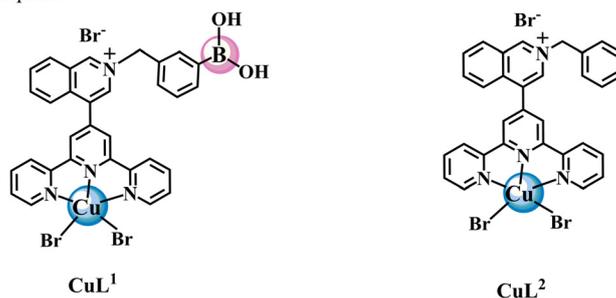
Synthesis and structural analysis

For these investigations, the bromide salts of **CuL^1** and **CuL^2** complexes were synthesized and studied as molecular receptors for a series of NTs, nucleosides and related analytes (Scheme 1).

CuL^1 includes two Lewis acids of different natures (B and Cu(ɪɪ) atoms) as binding sites for levodopa, and **CuL^2**, lacking phenylboronic acid, was prepared for comparison purposes. The synthesis was initiated with the preparation of 4-(terpyridine-4′-yl)isoquinoline, **1**, as we previously reported,[43] and subsequent treatment with 3-(bromomethyl)phenylboronic acid in dry CH_3CN under a N_2 atmosphere gave cationic ligand **L^1**. **L^2** was synthesized by the same synthetic path using benzyl bromide instead of a 3-(bromomethyl)phenylboronic acid.
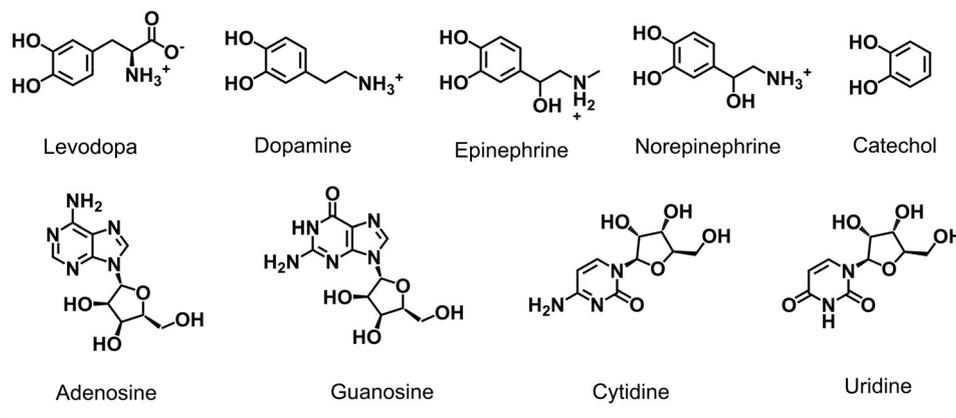
Intermediary **1** and the reported cationic ligands **L^1–L^2** were characterized by (^{1}H, ^{13}C, and ^{11}B) NMR spectroscopy, a positive scan of MS-ESI and ATR-IR. The expected numbers of (^{1}H and ^{13}C) NMR signals of the ligands were consistent with their chemical structures (Fig. S1–S6†). **CuL^1** and **CuL^2** complexes were synthesized by direct complexation with 1.10 equiv. of anhydrous $CuBr_2$ in CH_3CN at r.t. The bromide salts were obtained as green crystalline powders for both complexes and were pure according to MS-ESI and elemental analysis (C, H, and N). One charged state for **CuL^1**, monocationic species at m/z = 717.9822, corresponding to $[CuL^1Br_2]^+$ was clearly observed and isotopically resolved from its respective analysis by a positive scan of high-resolution ESI (Fig. S7†). MS-ESI(+)

Scheme 1 (A) Molecular receptors based on Cu(II)–boronic acid complexes employed in this study and (B) levodopa and related target analytes.

of **CuL²** also showed one charged state for a monocationic species at $m/z = 673.80$ corresponding to $[CuL^2Br_2]^+$ (Fig. S8†).

X-ray crystal structures were obtained for bromide salts of **CuL¹** and **CuL²**. Fig. 1 shows a molecular perspective view of these complexes. Tables S1–S5† contain the crystallographic data, hydrogen bond parameters within the crystal packing and selected distances/angles around Cu(II) and B atoms.

The X-ray crystal structure of **CuL¹** shows a complex with the formula $[CuL^1Br_2]Br·CHCl_3$ involving an sp²-hybridized B atom and a trigonal planar geometry $(\Sigma\sphericalangle(X–B–X) = 359.99°)$. B and Cu(II) atoms are separated by 11.07(4) Å. The single crystals of **CuL¹** for X-ray diffraction were obtained by diffusion of $CHCl_3$ vapor into a CH_3OH solution. As a result of this solvent, the boronic acid group was converted into a monomethyl boronic acid ester.

The methyl esterification of boronic acids from the crystallization solvent was also observed for Ir(III)–boronic acid complexes.[46] The B–O–H fragment is stabilized by a Br⁻ anion through a hydrogen bond (Table S2†). The crystal analysis showed that the Cu(II) atoms in **CuL¹** and **CuL²** possess a distorted square-pyramidal geometry with a $[CuN_3Br_2]$ coordination sphere.

The rings of quinolinium and central pyridine (from terpy) are significantly out of coplanarity for both crystals. For instance, the dihedral angle between the planes of quinolinium and central pyridine for **CuL¹** is 61.61°. This fact

suggests that although the complex has a paramagnetic Cu(II) atom, the fluorescence emission can be maintained, at least in residual form, because this Cu(II) atom is located at a long distance from the fluorescent unit. Furthermore, there is no coplanarity between the fluorescent quinolinium ring[47] and the Cu–terpy fragment. The distortion in the coplanarity between these rings seems to be primarily an electronic rather than a steric effect.[48]

Inspection of the crystal packings of **CuL¹** and **CuL²** reveals the presence of strong π···π stacking interactions between central pyridine and lateral pyridine rings of different molecules, as shown in Fig. S11.† These π···π interactions are not unexpected because they become more stable when Cu–terpy fragments point in opposite directions as has been reported in the area of inorganic crystal engineering.[49]

Photophysical and acid–base properties

Bromide salts of ligand **L¹** and cationic complexes **CuL¹** and **CuL²** possess good solubility in buffered (10 mM MOPS, pH = 7.4) pure water and follow well the Lambert–Beer law to 80 μM. Hence, concentrations within this range were used for further experiments.

The absorption and emission maxima $(\lambda_{ex} = 330)$ are compiled in Table 1 and the corresponding spectra of **L¹**, **CuL¹** and **CuL²** are shown in Fig. S12–S14.† Clearly, the **L¹** emission is almost three times higher than that observed for the **CuL¹**
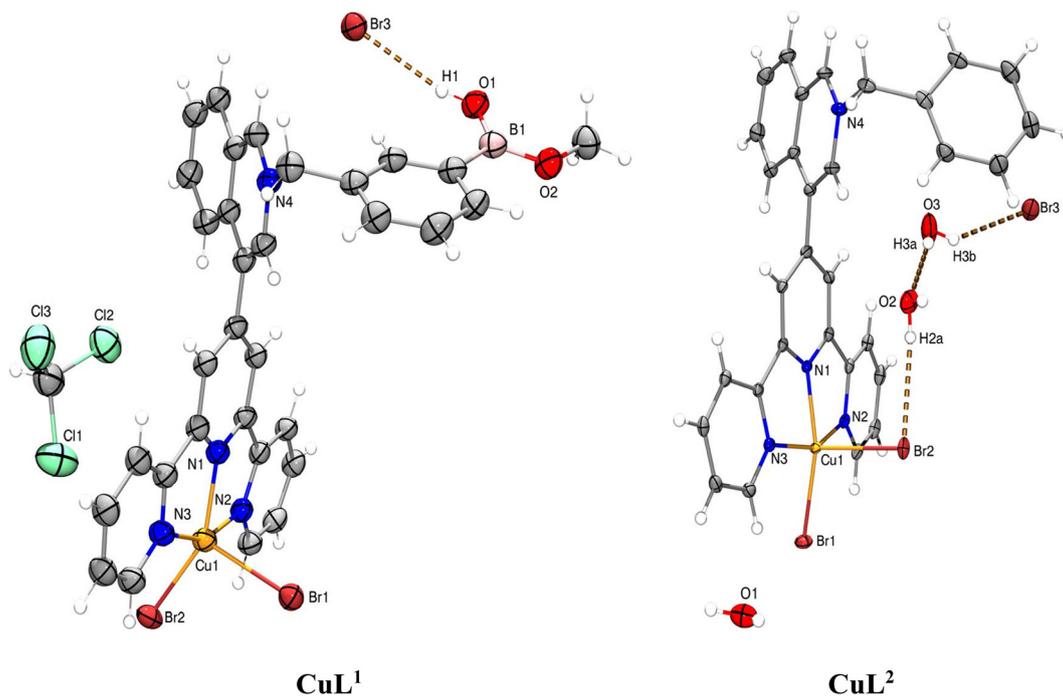
Fig. 1 ORTEP diagrams at 50% probability for bromide salts of Cu complexes. B−O−H···Br⁻ interaction in **CuL¹** is shown as dashed orange lines.

Table 1 Absorption and emission maxima (nm) of **L¹**, **CuL¹** and **CuL²** in water at pH = 7.40 and pK_a values estimated from fluorimetric titration experiments

Species	λ_{abs} (log ε)	Emission (λ_{ex})	Fluorimetric titration, pK_a (−B(OH)₂)
L¹	276 (4.22); 336 (3.83)	408 (330)	7.25 ± 0.07
CuL¹	330 (4.10); 343 (4.13)	407 (330)	6.29 ± 0.06
CuL²	334 (4.03); 344 (4.06)	403 (334)	—[a]

[a] Not calculated.

complex; this is not unexpected due to the paramagnetic effect of the Cu(ɪɪ) atom. However, it is interesting for our purposes that the Cu(ɪɪ) complexes still have residual emission, and this can be explained by the fact that the fluorescent quinolinium ring is outside the coplanarity of the Cu(ɪɪ) fragment. Furthermore, as observed in its crystalline structure, the Cu(ɪɪ) atom and the quinolinium–phenylboronic fragment are separated by a long distance of ~10 Å (*vide supra*).

The literature offers several fluorescent Cu(ɪɪ)-complexes that present large distances between the fluorescent unit and the Cu(ɪɪ)-fragment, such as Cu(ɪɪ)–benzimidazole[50] and Cu(ɪɪ)–terpy complexes.[51]

The pK_a values of phenyl boronic fragment of **L¹** and **CuL¹** can be estimated by the change in the fluorescence that occurs when the B atom converts from the sp²-trigonal to sp³-tetrahedral.[52] The pK_a values calculated from the titration curves are shown in Fig. 2 and Table 1.

The estimated pK_a of the −B(OH)₂ group of **CuL¹** is 6.29, which is an order of magnitude lower than the free ligand **L¹**

(pK_a = 7.25). For both species, the acid–base values are significantly lower than those of common receptors based on neutral arylboronic acids (phenylboronic acid pK_a = 8.90) for catechols.[53–55]

This finding is key to our objectives because it reveals that the −B(OH)₂ group in **CuL¹** is in its sp³-boronate form at pH = 7.40, which is the most active B-hybridization form to coordinate diols enabling levodopa recognition under "physiological" conditions.

Furthermore, it is well known that low pK_a values of arylboronic acids increase the affinity for diols.[53,56–58] In principle, this strongly acidified quinolinium–B(OH)₂ group is not unexpected because it is known that the cationic nature of the π electron-deficient quinolinium ring covalently appended to phenylboronic acid considerably reduces the pK_a values by up to two orders of magnitude as studied by Geddes with several (iso)quinolinium-nuclei bearing boronic acids for recognition of saccharides as well as CN⁻ and F⁻.[52,59–61]

The very low pK_a (**CuL¹**) value can only be explained by the coordination of **L¹** with the Cu(ɪɪ) atom, which results in a dramatic decrease in its pK_a value. To the best of our knowledge, this pK_a value is amongst the lowest reported for a phenylboronic acid derivative, and this study is the first to report the pK_a value of a phenylboronic acid appended to a Cu(ɪɪ)-complex. There are two examples in the literature based on Zn(ɪɪ)–boronate and Gd(ɪɪɪ)–boronate complexes with pK_a values between 4.60 and 7.33, respectively.[43,62]

An increase in the Lewis acidity of boronic acids is highly desired in the field of molecular recognition, and these low pK_a values demonstrate that the insertion of fragments of
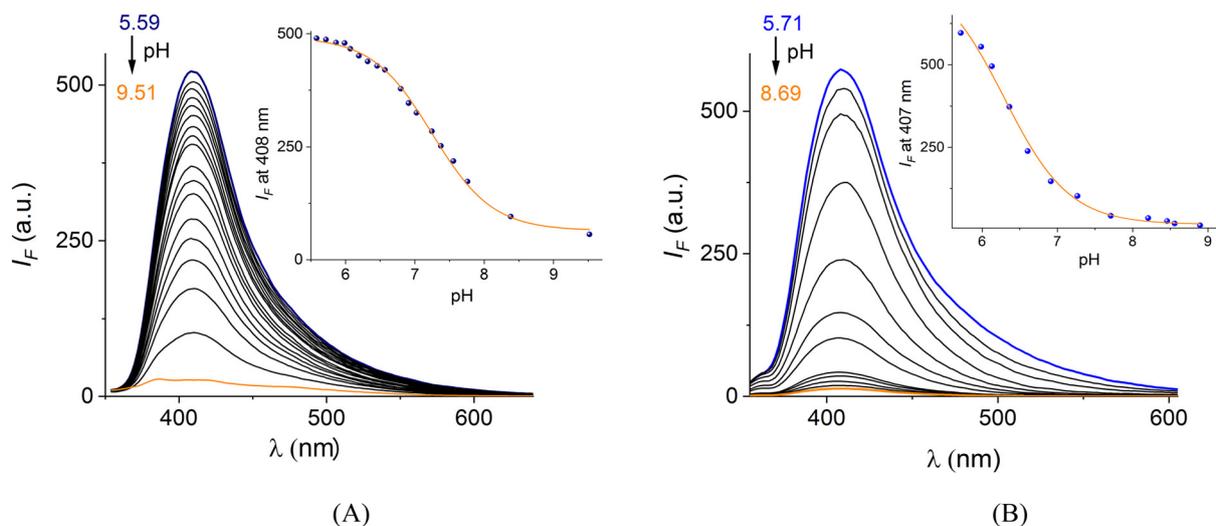
Fig. 2 Fluorescence spectra (λ_{ex} = 330 nm) of (A) L^1 (10 μM) and (B) CuL^1 (10 μM) in buffered aqueous solutions at different pH values. Insets: the observed pH-titration profile at the emission maximum of each species.

metal complexes within boronic acids can be a novel alternative.

Levodopa molecular recognition

Direct evidence of the high affinity of the CuL^1 complex towards levodopa was provided by electrospray ionization (ESI) mass studies, UV-vis measurements, ^{11}B NMR spectroscopy and EPR spectra. High-resolution ESI mass spectra were performed in the positive mode with water–EtOH (v/v, 1/1) solutions of CuL^1 (25 μM) in the absence and the presence of 1.1 equiv. of levodopa.

For the free complex CuL^1 only one charged state at m/z = 717.9822 corresponding to the monocationic species $[CuL^1Br_2]^+$ is clearly seen and isotopically resolved (Fig. 3A). The HRMS-ESI spectrum with levodopa showed only one species at m/z = 781.2455, which was also isotopically resolved.

This can be ascribed to the monocationic supramolecular complex 1:1, $\{[CuL^1 \cdot levodopa] \cdot EtOH\}^+$, as shown in Fig. 3B. The experimental signals, separated by 1.0 units, match very well the theoretical isotopic distribution for the supramolecular complex 1:1, and the multiplicity of this signal fits well with the presence of a B atom and a Cu atom with their corresponding isotopes. No Br atoms are observed, which suggests
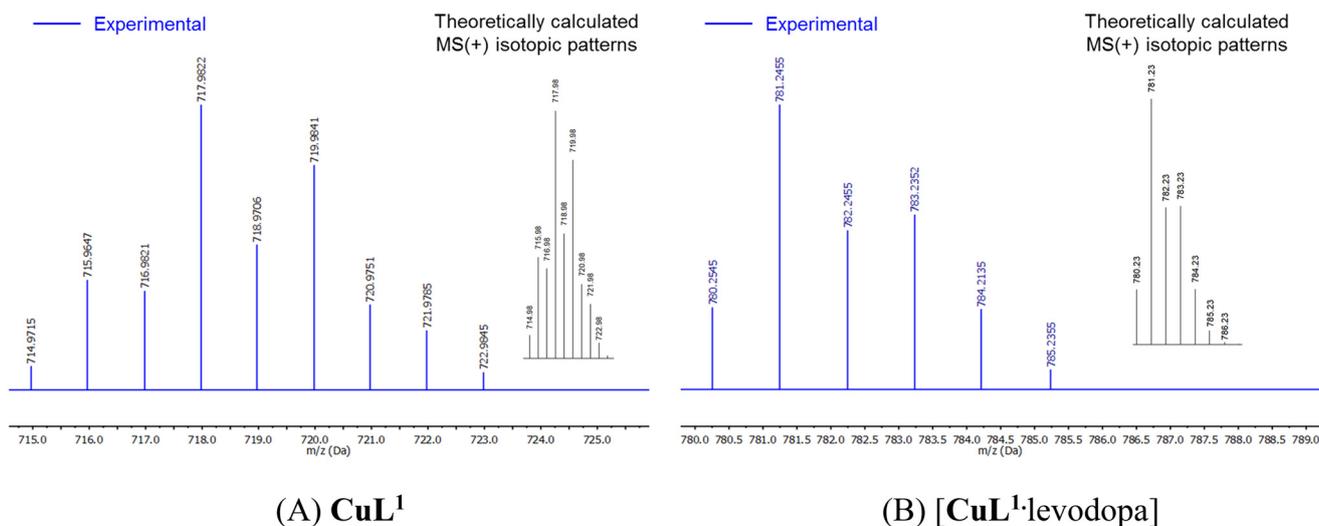

Fig. 3 Positive scan HRMS-ESI mass spectra of ethanolic aqueous solution (v/v, 9/1) of complex CuL^1 in (A) the absence and (B) the presence of 1.1 equiv. of levodopa. Inset: calculated isotopic distribution for monocationic complex $[CuL^1Br_2]^+$ and monocationic $\{[CuL^1 \cdot levodopa] \cdot EtOH\}^+$, 1:1 supramolecular complex.
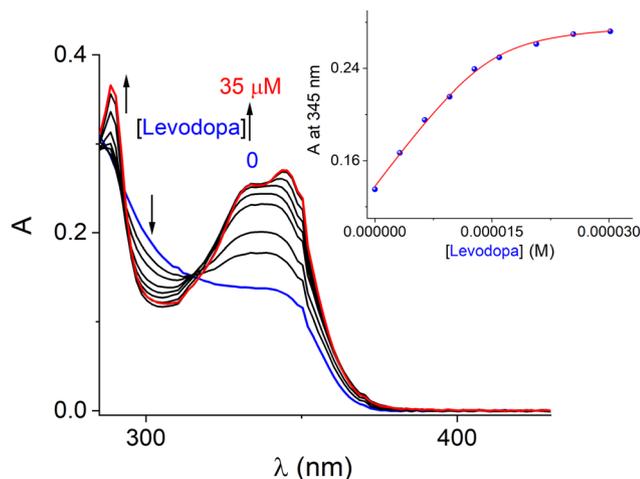
Fig. 4 Spectrophotometric titration of a buffered (10 mM MOPS at pH = 7.4) aqueous solution of **CuL**[1] (15 mM) by levodopa. The arrows show the direction of the spectral change. The inset shows the isotherm curve at 345 nm for increasing amounts of levodopa. The solid line was obtained by fitting the data to a 1 : 1 binding model.

that the monocharged species seen in the HRMS-ESI analysis corresponds to the species formed by the tri-cation of **CuL**[1] + boronate group −B(OH)$_3$ + carboxylate group from levodopa.

Fig. 4 displays the set of UV-vis spectra obtained when a buffered (pH = 7.4) aqueous solution of **CuL**[1] (15 μM) is titrated with levodopa (0–35 μM). Two isosbestic points at 296 and 318 nm were observed, which indicates that only two species (free form and complexed with levodopa) are in equilibrium. The inset shows the absorbance change at 345 nm ($\Delta A = 0.14$) on increasing the amount of levodopa. The spectrophotometric titration profile was practically saturated when the **CuL**[1]/levodopa ratio reached 1

equiv., suggesting a 1 : 1 stoichiometry. This UV-vis isotherm could be well fitted to a 1 : 1 binding model by a nonlinear least-square treatment to give an apparent binding constant of $K_{(1:1)} = (9.98 \pm 0.07) \times 10^5$ M^{-1}. HRMS-ESI and UV-vis experiments unambiguously confirm the binding of levodopa with **CuL**[1] in water.

Further evidence of interaction between **CuL**[1] and levodopa was sought through ^{11}B NMR and EPR experiments. Encouraged by reports of an *ortho*-carborane-based sensor for the detection of paramagnetic Cu(II) ions by ^{11}B NMR signals in D$_2$O,[63] we recorded the ^{11}B NMR spectra of free **CuL**[1] and **CuL**[1] + levodopa in CD$_3$OD–D$_2$O (v/v, 2/8). The ^{11}B NMR signal of the solution of the free **CuL**[1] is clearly observed at $\delta = 27.13$ ppm (Fig. 5A), and it can be assigned to a sp^2-hybridized B atom, consistent with its X-ray crystal structure. However, this value is upfield shifted compared to neutral phenylboronic acid ($\delta \sim 30$ ppm).[64] The ^{11}B NMR chemical shift ($\Delta\delta \sim 6$ ppm) can be ascribed to the strong acidification of the phenylboronic fragment in **CuL**[1] due to a combination of (1) the delocalized positive charge on the isoquinolinium ring as described in the literature,[43,52,64] and (2) the coordination of L[1] to the Cu(II) atom; a similar effect, a similar drop of pK_a value, has been documented for a Tb(III)–boronic acid complex.[62]

The strong acidification of boronic acid from **CuL**[1] was evidenced by the low calculated p$K_a = 6.29$ compared to neutral phenylboronic acid (p$K_a = 8.80$).[54] The addition of 5.0 equiv. of levodopa to a solution of **CuL**[1] provokes an upfield shift of the ^{11}B NMR signal at 8.77 ppm. This new signal can be ascribed to conversion of the B atom from the neutral sp^2 trigonal planar to the anionic sp^3 tetrahedral boronate form.[65]

The EPR spectrum of a frozen methanolic solution of **CuL**[1] (3.0 mM) shows an anisotropic signal with characteristic hyperfine bands of a Cu(II)–terpy complex involving values of $g_\perp = 2.075$ and $g_\parallel = 2.230$, as shown in Fig. 5B.[66]

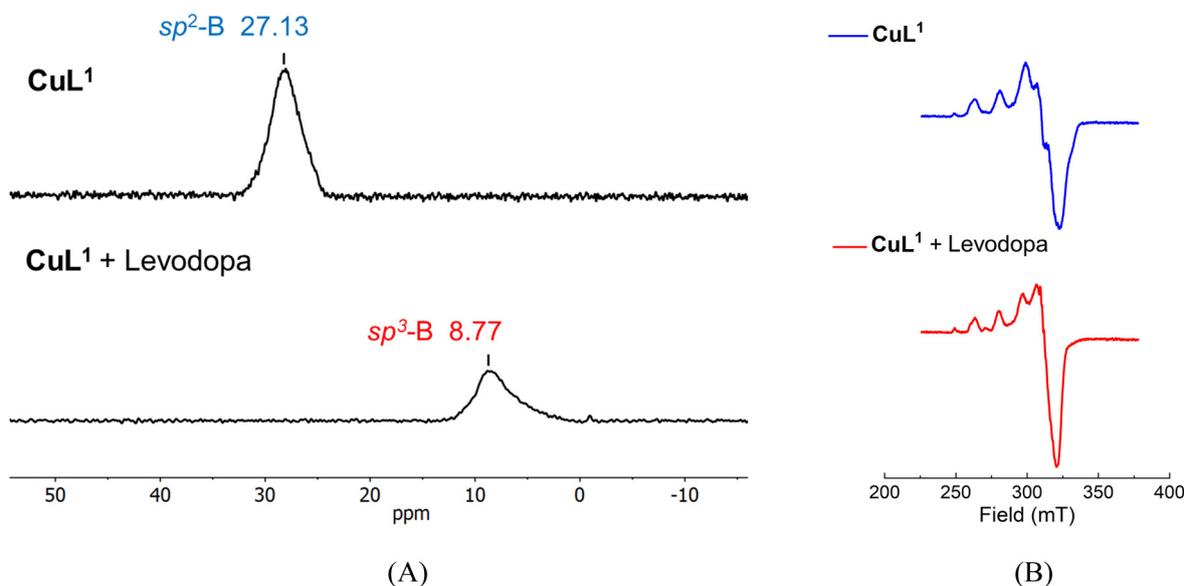
(A)

(B)

Fig. 5 (A) Change in ^{11}B NMR spectra (96 MHz) of **CuL**[1] (3.0 mM) in the absence and the presence of levodopa (15 mM) in CD$_3$OD–D$_2$O (v/v, 2/8). (B) X-band EPR spectra recorded at 70 K in methanol solutions of **CuL**[1] (3.0 mM) in the absence and the presence of levodopa (15 mM) (microwave frequency = 9.444 GHz, modulation amplitude = 0.0003 G).

These g values in the order of $g_\parallel > g_\perp > 2.0023$ correspond to a typical EPR spectrum for a Cu(II)–terpy with a square-based geometry, which is consistent with its X-ray structure. Furthermore, the $A_\parallel$ value of 162×10^{-4} cm^{-1} suggested that **CuL^1** has a square-pyramidal geometry ($A_\parallel = 154$–164×10^{-4} cm^{-1} for a square-based geometry).[66] On the other hand, the spectrum of the same solution containing 5.0 equiv. of levodopa shows an increase in the intensity of observed peaks and modestly modifies the spectral parameters ($g_\perp = 2.065$, $g_\parallel = 2.22$ and $A_\parallel = 156 \times 10^{-4}$ cm^{-1}). These results indicate that (1) the distorted square-pyramidal geometry practically remains with a $d_{x^2-y^2}$ ground state after binding levodopa and (2) the slight changes in the g and $A_\parallel$ values may be caused by the coordination of the $-CO_2^-$ group of the levodopa.

Interaction studies of Cu(II)–receptor with NTs by fluorescence spectroscopy

It is known that when catechol derivatives or diols are condensed with fluorescent boronic acids, their photophysical properties, such as intensity and emission maxima, are modified through several mechanisms. Such change provides a signal indicating boronate–diol esterification.[67,68]

Indeed, signaling mechanisms such as photoinduced electron transfer (PET), fluorescence resonance energy transfer (FRET) and photo-induced charge transfer (PICT) are efficient mechanisms for optical phenylboronic acid-based chemosensors of NTs and saccharides.[1,2,67]

Taking advantage of the fact that complex **CuL^1** emits residual fluorescence in pure water, we studied it as an intrinsic chemosensor to get a more sensitive optical response. Next, we analyzed the fluorescent selectivity of **CuL^1** towards a series of NTs.

Levodopa, epinephrine, norepinephrine, dopamine and related nucleosides such as adenosine, guanosine, cytidine and uridine ([analyte]$_{total}$ = 30 μM) were added to a buffered (10 mM MOPS at pH = 7.4) aqueous solution of **CuL^1** (10 μM) and the emission spectra (λ_{ex} = 330 nm) was recorded, as shown in Fig. 6A.

All nucleosides, catechols and dopamines gave a very low quenching response, $I_F < 10\%$ of its initial intensity I_0. Adding epinephrine/norepinephrine resulted in a modest decrease in intensity of *ca.* 25% but this quenching was considerably lower than that observed for levodopa. Among the studied NTs, levodopa displayed the greatest quenching effect, ~88%, as shown in Fig. 6B in Stern–Volmer terms.

This quenching response is not unexpected because the phenylboronic acid sensors typically show a quenching analytical response due to a photoelectron transfer (PET) mechanism when forming a sp^3 boronate–diol ester.[2,43,67]

For further insight into the chemosensing ability and to estimate the affinity of **CuL^1** toward levodopa and epinephrine, fluorimetric titration experiments were performed under the same conditions.

The profile with levodopa at the maximum of 407 nm (Fig. 7A) could be perfectly fitted to a 1:1 binding isotherm by a nonlinear least-squares treatment by eqn (1) to get an apparent binding constant of $K = (4.76 \pm 0.06) \times 10^6$ M^{-1} where ΔI_{obs} corresponds to the observed change of intensity, I_R is the intensity of **CuL^1**, ΔI_∞ is the change of intensity induced by the levodopa, and [A]$_T$ and [R]$_T$ are the total concentrations of the analyte and sensor **CuL^1**, respectively. K is the *apparent* binding constant for the 1:1 model.

$$\Delta I_{obs} = I_R + 0.5\Delta I_\infty$$
$$\left\{ [A]_T + [R]_T + \frac{1}{K} - \left[\left([A]_T + [R]_T + \frac{1}{K} \right)^2 - 4[R]_T[A]_T \right]^{0.5} \right\}$$

(1)

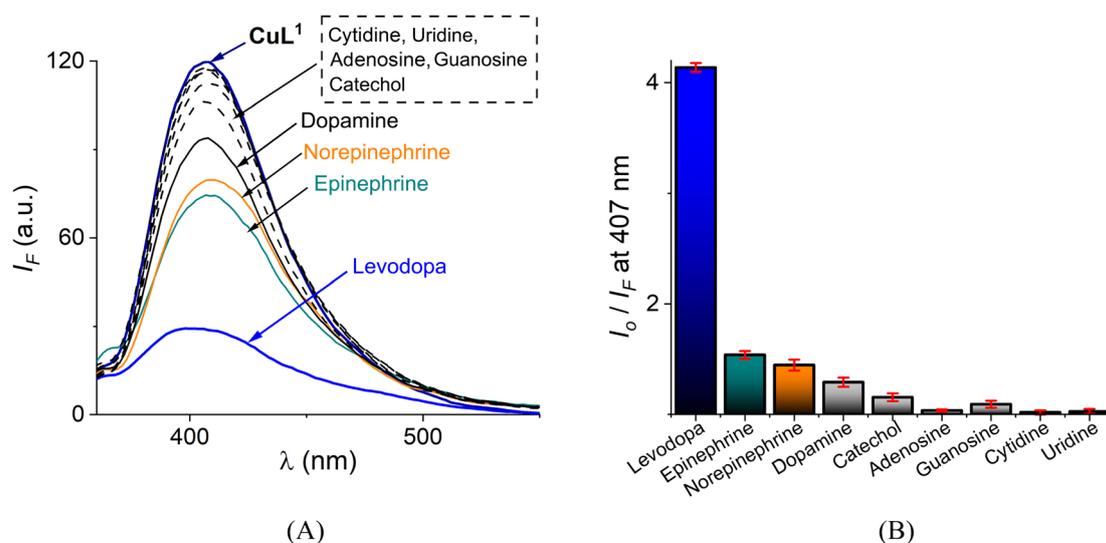The *apparent* complexation constant estimated using fluorescence is consistent with the value calculated using UV-vis

Fig. 6 (A) Effect in fluorescence spectra (λ_{ex} = 330 nm) and (B) the fluorescence quenching (I_0/I_F) at 407 nm of buffered (10 mM MOPS pH = 7.4 and 20 mM NaCl) aqueous solution of **CuL^1** (10 μM) upon the addition of several NTs, nucleosides, and catechol ([analyte]$_{total}$ = 30 μM) at pH = 7.4 (average of triplicate experiments).
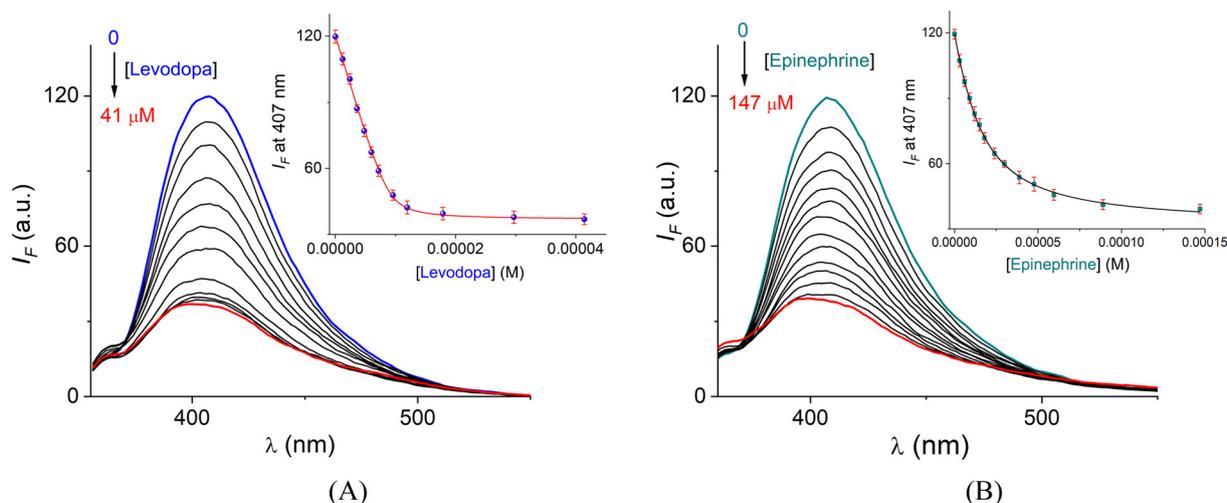
Fig. 7 Changes of emission spectra (λ_{ex} = 330 nm) of buffered (10 mM MOPS pH = 7.4 and 20 mM NaCl) aqueous solutions of **CuL¹** (10 μM) upon the addition of increasing amounts of (A) levodopa and (B) epinephrine at 25 °C. Inset: curve-fitting analysis of the fluorescence emission change at 407 nm (average of triplicate experiments). The solid line was obtained by fitting the experimental data to a 1 : 1 model.

(*vide supra*), indicating that the complexation **CuL¹**·levodopa practically takes place in the ground state.

The *apparent* binding constants for epinephrine (Fig. 7B), norepinephrine, dopamine, catechol and nucleosides (adenosine, guanosine, cytidine, uridine and ʟ-Tyr, analytes studied for comparison purposes) were calculated under the same conditions. The *K* values are compiled in Table 2, and their corresponding fitted fluorimetric titration profiles at 407 nm are shown in Fig. 8A and B. In all cases, good fits to the 1 : 1 binding model scheme were observed.

The tight binding of **CuL¹** toward catecholamines over nucleosides can be assigned to the higher affinity of boronic acids to the aromatic catechol fragments over that to the aliphatic 1,2-diol groups of ribose.[43]

ʟ-Tyr showed the lowest affinity among all the diols studied because of the lack of a catechol ring.

Analysis of the values in Table 2 shows that the affinity of **CuL¹** for levodopa is 3–4 orders of magnitude greater than that of nucleosides/ʟ-Tyr and at least 2 orders of magnitude greater than those of the rest of the NTs including epinephrine (Fig. 8C), which is a common interfering species.

Such levodopa affinity/selectivity for a metal-based chemosensor in water is still rare. To the best of our knowledge, the

affinity constant of **CuL¹** toward levodopa is the largest among the known synthetic receptors for this neurotransmitter in water (Table S6†). For example, this affinity is two orders of magnitude larger than that of organic receptors with a three-point recognition[39] or receptors based on boronic acid appended Zn(ɪɪ)-complexes that include two-point recognition.[38,43]

Complex **CuL¹** has a tighter affinity for levodopa compared to the related ZnL¹ complex (Table S6†), previously reported by us.[43] In principle, the higher affinity of levodopa for the **CuL¹** complex can be attributed to the fact that the Cu(ɪɪ) atom is more acidic in terms of Lewis acidity compared to the Zn(ɪɪ) atom, which should induce stronger coordination with the carboxylate and amine groups from levodopa.[45] Furthermore, the Cu(ɪɪ) atom has a higher versatility in its coordination geometry compared to Zn(ɪɪ) due to the Jahn–Teller effect, which stabilizes multiple coordination modes, including the chelate mode.[69]

The molecular recognition of **CuL¹** for levodopa in pure water is also remarkable because some receptors require organic co-solvents to work.

The main structural difference of levodopa compared to the rest of the NTs is the $-CO_2^-$ group. Therefore, the coordination

Table 2 Apparent binding constants $K_{1:1}$ (M^{-1}) for Cu(ɪɪ)-complexes (10 μM) with NTs, nucleosides and some comparative analytes in buffered aqueous solution at pH = 7.4

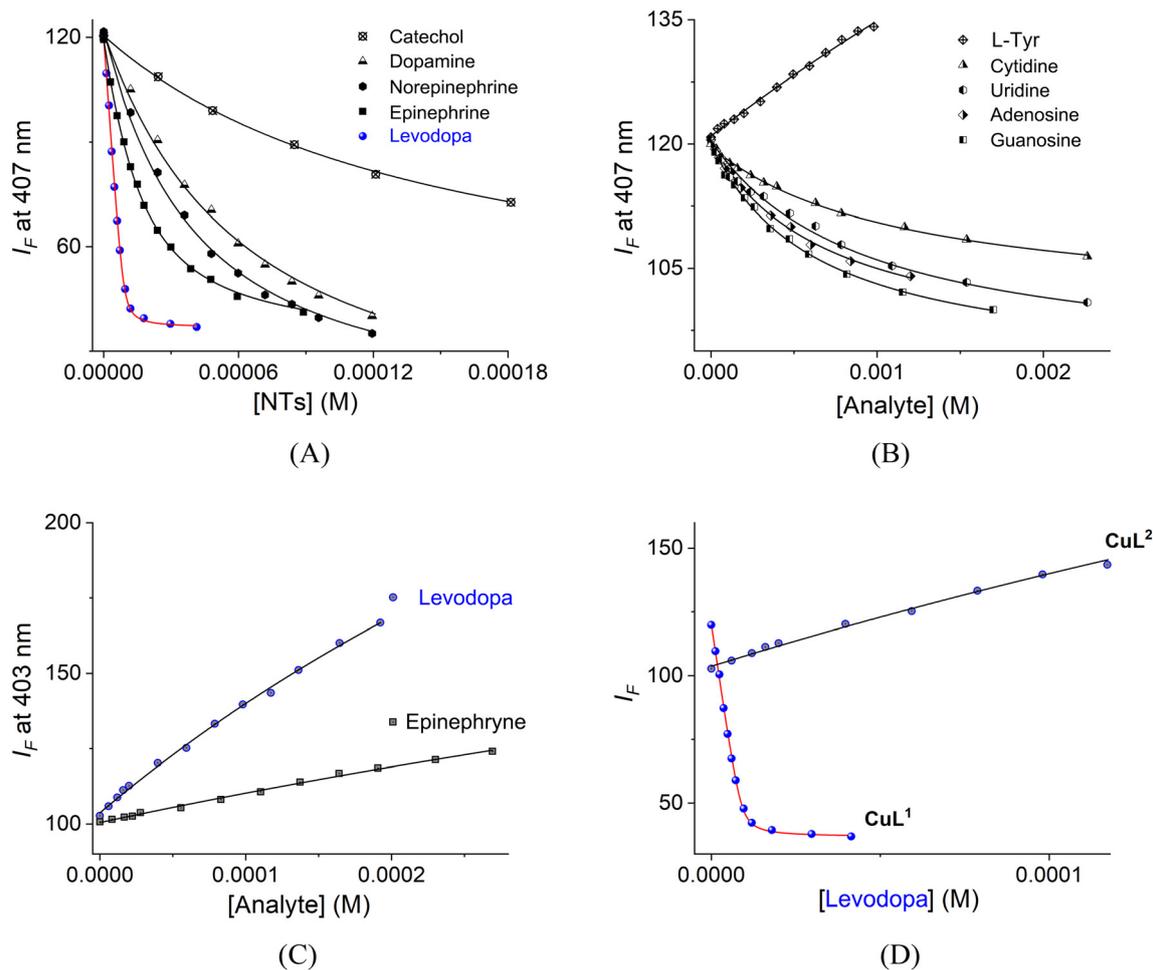| Analytes	**CuL¹**, $K_{1:1}$	Analytes	**CuL¹**, $K_{1:1}$	Analytes	**CuL²**, $K_{1:1}$
Levodopa	$(4.76 \pm 0.06) \times 10^6$	Adenosine	$(1.46 \pm 0.09) \times 10^3$	Levodopa	$(1.37 \pm 0.09) \times 10^3$
Epinephrine	$(9.15 \pm 0.11) \times 10^4$	Guanosine	$(1.59 \pm 0.08) \times 10^3$	Epinephrine	a
Norepinephrine	$(2.99 \pm 0.08) \times 10^4$	Cytidine	$(8.71 \pm 0.06) \times 10^2$	Norepinephrine	a
Dopamine	$(1.82 \pm 0.10) \times 10^4$	Uridine	$(1.01 \pm 0.12) \times 10^3$	Dopamine	a
Catechol	$(7.20 \pm 0.05) \times 10^3$	ʟ-Tyr	$(3.28 \pm 0.05) \times 10^2$	Catechol	a

^{a} Not calculated.

Fig. 8 Fluorimetric titrations of buffered aqueous solutions of (A and B) **CuL**^{1} (10 μM, λ_{ex} = 330 nm) and (C) **CuL**^{2} (10 μM, λ_{ex} = 338 nm) upon the addition of increasing amounts of NTs, nucleosides and related analytes at pH = 7.4 and 25 °C. (D) Fluorimetric titration profiles of **CuL**^{1} and **CuL**^{2} with levodopa. The solid lines were obtained in all instances by fitting the curves to eqn (1).

of this anionic group to the Cu(II) atom can act as a second recognition point, which drives the high affinity. In terms of pertinent equilibrium constants, the stability of Cu(II)–receptor–analyte decreases according to the sequence: levodopa ≫ epinephrine ~ norepinephrine > dopamine ≫ nucleosides and L-Tyr.

To verify that boronate–catechol condensation is present in the binding process between **CuL**^{1} and levodopa, we measured the affinity of levodopa toward the reference complex **CuL**^{2}, which lacks phenylboronic acid, by a fluorimetric titration under the same conditions as for **CuL**^{1} (Fig. 8D).

The affinity of levodopa toward **CuL**^{2} is three orders of magnitude lower compared to that of **CuL**^{1} and, interestingly, the analytical response is a modest turn-on of the emission (Fig. S15†), indicating: (1) coordination of levodopa with the Cu(II) atom is evidenced by the EPR spectra; and (2) the quenching emission of the aqueous solution of **CuL**^{1} induced by the binding with levodopa must be due to a PET mechanism, which is originated by the formation of sp^3 boronate that is not observed with the reference **CuL**^{2} complex.

The reversibility of the boronic acid–diol interaction is a key aspect of molecular recognition because it serves as a basis for understanding and improving the sensing response of the target analyte.

For practical applications, fluorescent levodopa receptors are required to work in the presence of coexistent interfering ions and molecules in biological and complex samples. Next, a selectivity experiment of **CuL**^{1} (10 μM) towards typical interfering species in urine and blood plasma ([interference] = 2.0 mM each: creatinine, urea, L-proline, D-glucose, ATP, NH$_4$Cl, MgCl$_2$, KCl and NaCl) was performed in water at physiological pH.

Overall, the addition of these interferences induced a negligible emission shift, which is <3% of the initial intensity (Fig. 9A). It should be noted that the interfering species are present in the millimolar concentration range, which is a higher concentration than that commonly found in real samples. Outstandingly, Fig. 9B shows that the quenching effect at 407 nm induced by levodopa is not affected by the background species of the blood plasma and urine supporting the sensing/selectivity performance in this system.
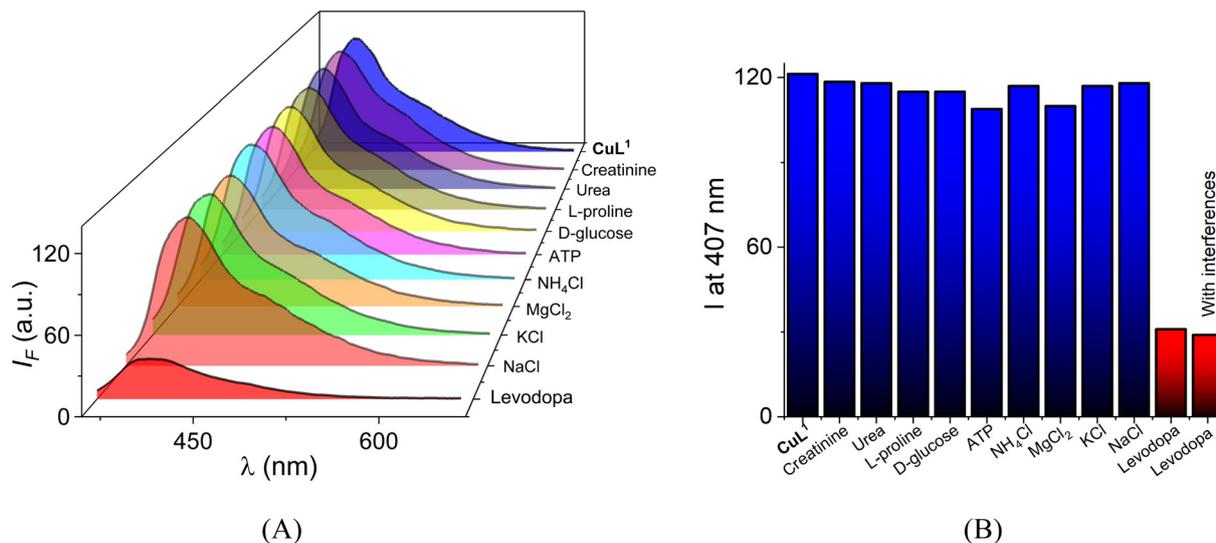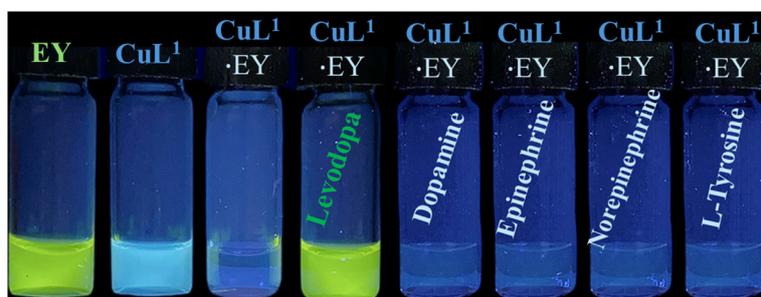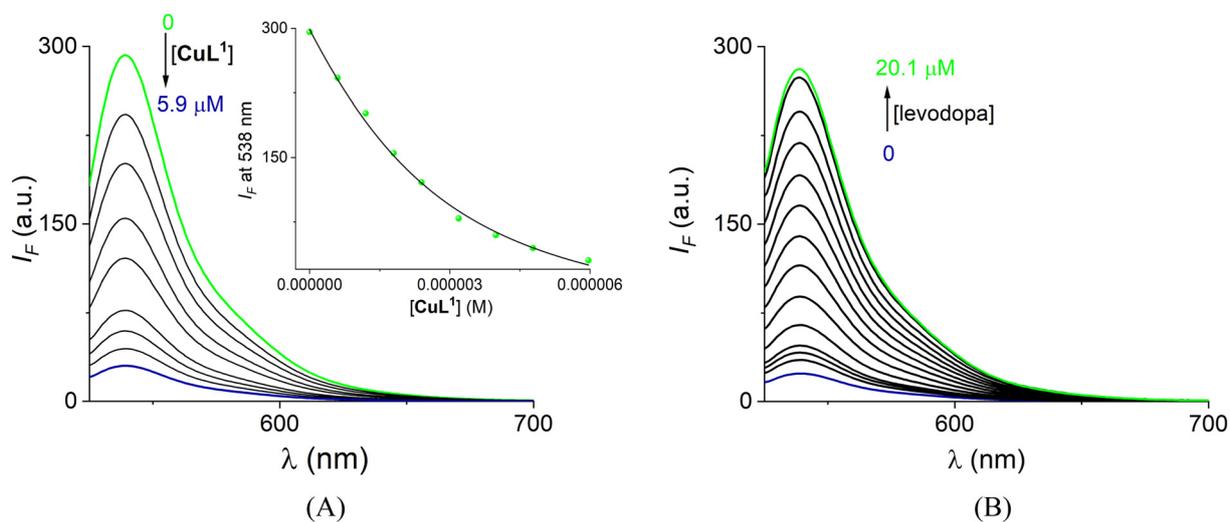
Fig. 9 Fluorescence spectra (λ_{ex} = 330 nm) (A) and intensities at 407 nm of aqueous solutions of **CuL¹** (10 μM) at pH = 7.4 with several blood plasma and urine components ([Interference] = 2.0 mM each) (B).

Fig. 10 Changes in the emission (λ_{ex} = 515 nm) spectra of (A) EY (2.0 μM) upon the addition of **CuL¹** (0–6.0 μM). The inset shows the titration profile at 538 nm, and the solid line was obtained by fitting it to a 1 : 1 binding model. (B) Changes in the emission (λ_{ex} = 515 nm) spectra of complex EY·**CuL¹** (1/3 equiv.) upon the addition of levodopa (0–20.1 μM) in an aqueous solution at pH = 7.4 (10 mM MOPS). (C) Color change of solutions under irradiation at 366 nm UV light.

Sensing ensemble for optical detection of levodopa

A key part of the optical receptor design is the transduction of the molecular recognition into an efficient optical signal. Considering the high affinity of levodopa for **CuL¹**, we developed a visual sensing ensemble for the selective detection of levodopa built with **CuL¹** and a commercial fluorescent indicator, eosin-Y (EY).

It is well documented that the interaction of organic fluorescent dyes bearing a carboxylate group (*e.g.* EY) with transition d^n metal complexes (n = 1–9) alters their emission properties; typically, the interaction quenches the excited state through an electron transfer or an energy transfer.[69]

As a result, fluorescent sensing of analytes with high affinity for the transition metal complex is achieved by restoring the dye's emission when it is released to the solution by the action of the analyte.

Next, we investigated the affinity of the anionic dye EY (2.0 μM) with **CuL¹** using a fluorimetric titration experiment (Fig. 10A) upon excitation at 515 nm in buffered water at pH = 7.4.

On **CuL¹** addition, the fluorescence of the dye is progressively quenched, which reflects the coordination with the Cu(II) atom of the complex. The titration profile at 538 nm showed that the almost total quenching of the EY occurs on the addition of *ca.* 3 equiv. of **CuL¹**. These data were well fitted to the species of 1 : 1 stoichiometry to give a binding constant of $K_{(EY)} = (6.71 \pm 0.11) \times 10^5$ M^{-1}.

The affinity of **CuL¹** for EY is less than the affinity calculated for levodopa, making this an ideal ensemble for a visual sensing system by an indicator displacement assay (IDA).[70] In principle, the selectivity of an IDA is suitable when the dye has a slightly lower affinity than the target analyte but a more considerable affinity than other competitive analytes.[71]

Upon the addition of levodopa to a buffered water solution of the ensemble EY·**CuL¹** (1/3.0 equiv.), the dye is rapidly displaced, hypothetically *via* the discoordination of the CO_2^- group (from EY) of the Cu(II) atom and its green emission is restored practically entirely, as shown in Fig. 10B. The strong visible fluorescence of EY allows the real-time and selective sensing of levodopa by the naked eye under UV light, as shown in Fig. 10C. The green emission of EY is totally quenched by the interaction with **CuL¹**. The resulting solution presents a faint blue emission that can be reflected by the fluorescent unit (quinolinium ring) of the Cu(II)–boronate receptor, which is not altered. Subsequently, the addition of 10 equiv. (20.1 μM) of levodopa to the aqueous solution of the ensemble EY·**CuL¹** restores 97% of the original intensity emission of EY at 538 nm.

DFT theoretical section

Finally, to gain further insight into the cooperative binding mode of **CuL¹** with the catechol-based NTs, density functional theory calculations were carried out for the corresponding supramolecular complexes 1 : 1.
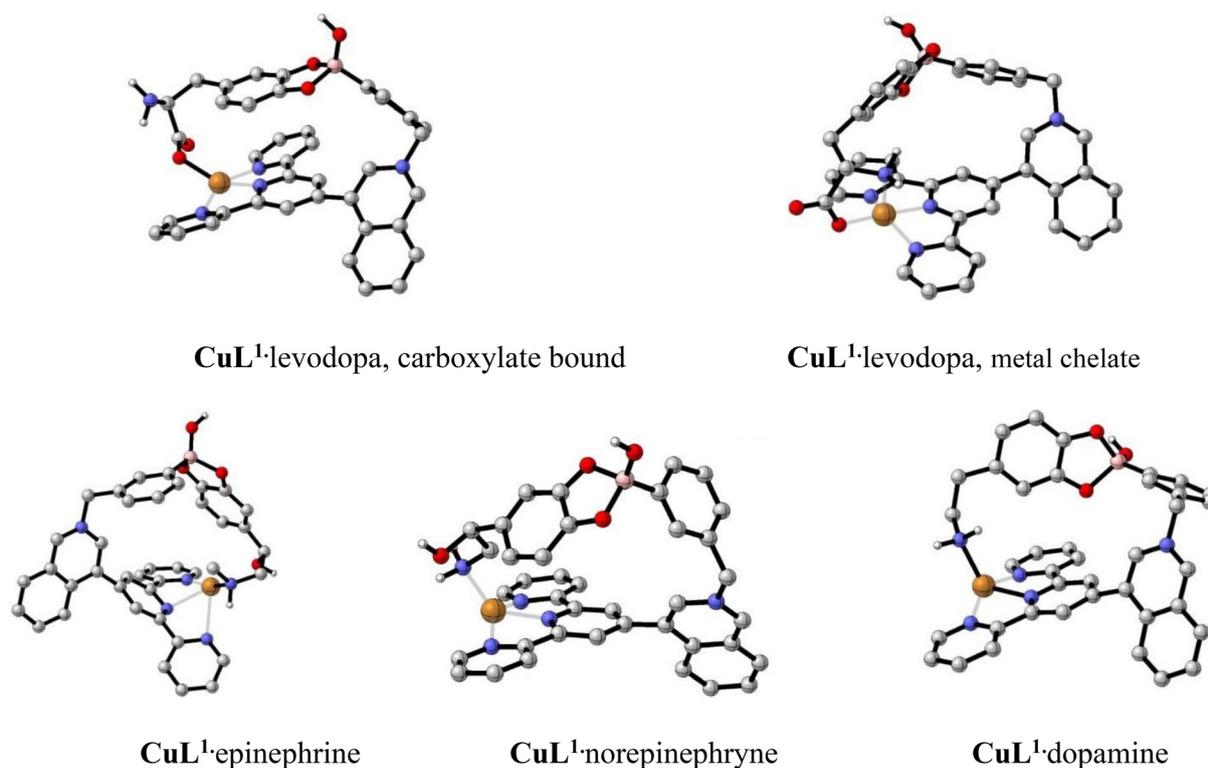

CuL¹·levodopa, carboxylate bound

CuL¹·levodopa, metal chelate

CuL¹·epinephrine

CuL¹·norepinephryne

CuL¹·dopamine

Fig. 11 Optimized geometries of all four complexes **CuL¹**-NTs at the ωB97XD/LANL2DZ level of theory.

Table 3 Relative interaction energies to copper [kcal mol^{-1}] calculated at the ωB97XD/LANL2DZ level of theory

Neurotransmitter bound to **CuL^1**	E_{bind} [kcal mol^{-1}]
Dopamine	0.000
Epinephrine	228.041
Norepinephrine	199.437
Levodopa, carboxylate bound	276.693
Levodopa, metal chelate	290.703

All calculations were carried out with the Gaussian 16 suite of programs at the ωB97XD/LANL2DZ level of theory.[72] All compounds were optimized at the mentioned level of theory, and no imaginary frequencies were obtained, thus confirming the presence of minima on the potential energy surface. Their optimized geometries are shown in Fig. 11. Every complex shows a four-coordinate geometry around the Cu(II) atom, with an open site opposed to the ligand that could in principle be filled with a water molecule in solution.

In order to account for the observed selectivity of the analytes (NTs), binding energies to Cu complexes for every analyte were calculated as energy differences at the complex optimized geometry according to eqn (2).

$$E_{bind} = (E_{lig} + E_{Cu(II)}) - E_{cplx} \qquad (2)$$

where E_{lig} is the energy of the analyte at the optimized geometry of the complex, $E_{Cu(II)}$ is the energy of the Cu(II) ion, and finally, E_{cplx} is the energy of the optimized **CuL^1**–NT complex. The E_{bind} results are listed in Table 3.

In general, calculated E_{bind} values correlate well with the observed experimental trend of a higher selectivity of **CuL^1** towards levodopa, involving a cooperative interaction between an ester boronate-catechol and a coordination bond of the $-CO_2^-$ group with the Cu(II) atom.

For the case of levodopa, the chelate coordination was also considered theoretically, in which the $-NH_2$ group is directly coordinated to Cu(II) together with the carboxylate group (Fig. 11B). The resulting structure is 14.01 kcal mol^{-1} more stable than the corresponding isomer shown in Fig. 11A. The binding energy as calculated by means of eqn (2) is 261.05 kcal mol^{-1}.

Conclusions

We have developed the first example of a fluorescent Cu(II)–terpy complex bearing an intramolecular phenylboronic acid strongly acidified (**CuL^1**) for optical recognition of levodopa with exceptionally strong affinity ($K = 4.76 \times 10^6$ M^{-1}) and selectivity over structurally related neurotransmitters such as dopamine, epinephrine, norepinephrine and nucleosides in pure water at physiological pH. The affinity of levodopa for **CuL^1** is the highest compared to all boronic acid-based molecular receptors reported until now.

The addition of levodopa to an aqueous solution of the cationic **CuL^1** receptor induces a remarkable turn-off signal

in the micromolar concentration range. Spectroscopic outputs by ^{11}B NMR, UV-vis, EPR, fluorescence titration experiments, HRMS-ESI measurements and X-ray crystal structure, and DFT calculations showed that levodopa is bound to the **CuL^1** receptor in a 1 : 1 mode through two-point recognition that includes a boronate–catechol complexation and a coordination bond of the carboxylate anion (levodopa) to the Cu(II) atom.

The combination of the receptor **CuL^1** with eosin-Y can be effectively used as an indicator displacement assay to detect levodopa with the naked eye through a turn-on green fluorescence signal that is not observed for the rest of the neurotransmitters.

Overall, these results highlight the use of novel fluorescent and water-soluble metal receptors based on two different Lewis acids with analytical applications for the selective sensing of catecholamines with medical and biochemical relevance.

Experimental section

The general experimental procedures, equipment and chemicals are described in the ESI.† Intermediate **1** and ligands **L$^{1-2}$** were prepared according to the established synthetic procedures in the literature.[43]

General synthesis path for the Cu complexes

The corresponding ligand **L^1** or **L^2** and 1.10 equiv. of the CuBr$_2$ salt were placed in a balloon flask with 5.0 mL of dry CH$_3$CN and stirred for 24 h. at r.t. to give a green solid (in both cases). The solvent was removed under reduced pressure; the precipitate was washed with cold ethyl ether–acetone (10 mL, v/v, 8/2) and dried under vacuum for ~2 h to give the bromide salt of the corresponding Cu(II) complex.

Synthesis of compound CuL^1

Following the general path, the ligand **L^1** (43.0 mg, 0.08 mmol) and CuBr$_2$ (18.55 mg, 0.088 mmol) were reacted to obtain **CuL^1**. Yield: 56.71 mg (95.0%). Green single crystals of **CuL^1** for X-ray diffraction analysis were obtained by the diffusion of CHCl$_3$ vapor into a CH$_3$OH concentrated solution at r.t. after 4 days.

HRMS-ESI$^+$ (m/z): calculated for $[C_{31}H_{24}BBr_2CuN_4O_2]^+$: 717.9613, found: 717.9822. ATR-IR ν (cm^{-1}): 3420 (m, ν (B–O)), 3218(br), 3010(w), 1605(m), 1366(s, ν (B–O)), 1090 (m, ν (B–C)), 1020(m), 791(s), 413(m). Anal. calcd for crystalline sample: C$_{33}$H$_{27}$BBr$_{2.54}$Cl$_{3.46}$CuN$_4$O$_2$; C, 43.48; H, 2.99; N, 6.15. Found: C, 43.20; H, 3.05; N, 6.18. EPR (CH$_3$OH, 77 K): $g_\perp = 2.075$, $g_\parallel = 2.236$.

Synthesis of compound CuL^2

Following the general path, the ligand **L^2** (50.0 mg, 0.09 mmol) and CuBr$_2$ (23.34 mg, 0.10 mmol) were reacted to obtain **CuL^2** as a green solid. Yield: 63.91 mg (90.0%). Deep-blue single

crystals of **CuL²** for X-ray diffraction analysis were obtained by slow evaporation from CH_3CN–H_2O (v/v, 9/1) solution after 1 week.

MS-ESI(+) (m/z): calculated for $[C_{31}H_{23}Br_2CuN_4]^+$: 673.96, found: 673.80. ATR-IR ν (cm^{-1}): 3426(br), 2953–2928(m), 1729(m), 1602(s), 1397(m), 793(s), 415(m). Anal. calcd for crystalline sample: $[C_{31}H_{23}Br_3CuN_4]\cdot3(H_2O)$; C, 46.03; H, 3.61; N, 6.93. Found: C, 43.00; H, 3.67; N, 6.89. EPR (CH_3OH, 77 K): $g_\perp$ = 2.057, $g_\parallel$ = 2.245.

Fluorescence. Fluorimetric titration experiments (λ_{ex} = 330 nm) were carried out by adding aliquots of stock solutions of the analyte to a buffered aqueous solution (10 mM MOPS, pH 7.4, 20 mM NaCl) of the corresponding Cu complex (10 μM). After adding the analyte, the solution was equilibrated by magnetic stirring for 2 min, before recording the emission spectrum using a quartz cuvette.

¹¹B NMR and spectrophotometric titration experiments. For ¹¹B NMR measurements, the spectra were recorded at 96 MHz in CD_3OD. An aliquot of concentrated stock solution of levodopa was added directly to **CuL¹** (10 mM) solution at 25 °C using quartz NMR tubes.

Crystallographic experiments. The relevant details of the crystals **CuL¹** and **CuL²** data collection and structure refinement can be found in Table S1.† Data for both crystals were collected on a Bruker APEX II CCD diffractometer at 100 K, using Cu-Kα radiation (k = 1.54178 Å) for **CuL¹** and Mo-Kα radiation (k = 0.71073 Å) for **CuL²** from an Incoatec ImuS source and a Helios optic monochromator. Suitable crystals were coated with hydrocarbon oil, picked up with a nylon loop, and mounted in the cold nitrogen stream of the diffractometer. Frames were collected using ω scans and integrated with SAINT.[73] Multi-scan absorption correction (SADABS) was applied. The structures were solved by direct methods and refined using full-matrix least-squares on F2 with SHELXL-2018v[74] using the SHELXLE GUI.[75] The occupational and positional disorder was modeled using EADP, SADI and ISOR instructions implemented in SHELXLE GUI,[75] and the occupations were refined using a free variable The hydrogen atoms of the C–H bonds were placed in idealized positions, the hydrogens of O–H moiety and the hydrogens of water molecules were found in the map of residual density, and their position was refined with $U_{iso} = aU_{eq}$ (where a is 1.5 for –CH_3 and –OH moieties and 1.2 for others). **CuL¹** crystallized in a monoclinic system in the $P2(1)/n$ space group. The crystal was refined as a 3-component twin with two BASF refined parameters (0.33600 and 0.16809). **CuL¹** presents an occupational disorder due to an incomplete substitution of the halogen atoms between bromide and chloride atoms; the ratio of the occupation refined was 54/46 for Br/Cl atoms labeled as Br4 and Cl4. **CuL²** crystallized in a monoclinic system in the P2(1)/c space group as a trihydrate salt, where one water molecule presented a positional disorder that was modeled in two positions; the majority occupation was 56% probability.

The molecular graphics were prepared using POV-RAY[76] and GIMP[77] programs.

Data availability

Crystallographic data for compounds **CuL¹** and **CuL²** have been deposited at the Cambridge Crystallographic Data Centre under CCDC 2340947 and 2340948.†

Conflicts of interest

There are no conflicts to declare.

Acknowledgements

References

1 T. Pradhan, H. S. Jung, J. H. Jang, T. W. Kim, C. Kang and J. S. Kim, Chemical sensing of neurotransmitters, *Chem. Soc. Rev.*, 2014, **43**, 4684–4713.

2 Z. Guo, I. Shin and J. Yoon, Recognition and sensing of various species using boronic acid derivatives, *Chem. Commun.*, 2012, **48**, 5956–5967.

3 H. Ge, Q. Ye, T. Zou, D. Zhang, H. Liu and R. Yang, Recent progress of molecular fluorescent probes with multi-recognition sites enable sensitive and selective analysis, *TrAC, Trends Anal. Chem.*, 2024, **174**, 117685.

4 M. Chemchem, A. Chemchem, B. Aydıner and Z. Seferoğlu, Recent advances in colorimetric and fluorometric sensing of neurotransmitters by organic scaffolds, *Eur. J. Med. Chem.*, 2022, **244**, 114820.

5 K. S. Hettie and T. E. Glass, Coumarin-3-aldehyde as a scaffold for the design of tunable PET-modulated fluorescent sensors for neurotransmitters, *Chem. – Eur. J.*, 2014, **20**, 17488–17499.

6 P. Jana and S. Bandyopadhyay, Optical sensor arrays for the detection of neurotransmitters, *Analysis Sensing*, 2024, **4**, e20230099.

7 Y. Ou, A. M. Buchanan, C. E. Witt and P. Hashemi, Frontiers in electrochemical sensors for neurotransmitter detection: Towards measuring neurotransmitters as chemical diagnostics for brain disorders, *Anal. Methods*, 2019, **11**, 2738–2755.

8 F. Ghasemi, M. R. Hormozi-Nezhad and M. Mahmoudi, Identification of catecholamine neurotransmitters using

fluorescence sensor array, *Anal. Chim. Acta*, 2016, **917**, 85–92.

9 N. Chauhan, S. Soni, P. Agrawal, Y. P. S. Balhara and U. Jain, Recent advancement in nanosensors for neuro-transmitters detection: Present and future perspective, *Process Biochem.*, 2019, **91**, 241–259.

10 Y. Misu, Y. Goshima and T. Miyamae, Is DOPA a neuro-transmitter?, *Trends Pharmacol. Sci.*, 2002, **23**, 262–268.

11 T. Nagatsu and H. Ichinose, Molecular biology of catechol-amine-related enzymes in relation to Parkinson's disease, *Cell. Mol. Neurobiol.*, 1999, **19**, 57–66.

12 Y. C. Chou, C. I. Shih, C. C. Chiang, C. H. Hsu and Y. C. Yeh, Reagent-free DOPA-dioxygenase colorimetric bio-sensor for selective detection of L-DOPA, *Sens. Actuators, B*, 2019, **297**, 126717.

13 S. D. Niyonambaza, P. Kumar, P. Xing, J. Mathault, P. De Koninck, E. Boisselier, M. Boukadoum and A. Miled, A review of neurotransmitters sensing methods for neuro-engineering research, *Appl. Sci.*, 2019, **9**, 1–31.

14 K. J. Broadley, The vascular effects of trace amines and amphetamines, *Pharmacol. Ther.*, 2010, **125**, 363–375.

15 J. Kim, B. Raman and K. H. Ahn, Artificial receptors that provides a preorganized hydrophobic environment: A bio-mimetic approach to dopamine recognition in water, *J. Org. Chem.*, 2006, **71**, 38–45.

16 Z. Wu, M. Li, H. Fang and B. Wang, A new boronic acid based fluorescent reporter for catechol, *Bioorg. Med. Chem. Lett.*, 2012, **22**, 7179–7182.

17 D. Merims and N. Giladi, Dopamine dysregulation syn-drome, addiction and behavioral changes in Parkinson's disease, *Parkinsonism Relat. Disord.*, 2008, **14**, 273–280.

18 J. E. Hardebo and C. Owman, Enzymatic barrier mecha-nisms for neurotransmitter monoamines and their precur-sors at the blood–brain interface, *Ann. Neurol.*, 1980, **8**, 1–11.

19 J. Zhang, F. R. Qu, A. Nakatsuka, T. Nomura, M. Nagai and M. Nomoto, Pharmacokinetics of L-dopa in plasma and extracellular fluid of striatum in common marmosets, *Brain Res.*, 2003, **993**, 54–58.

20 K. Hyland and P. T. Clayton, Aromatic L-amino acid decar-boxylase deficiency: diagnostic methodology, *Clin. Chem.*, 1992, **38**, 2405–2410.

21 F. Del Bello, M. Giannella, G. Giorgioni, A. Piergentili and W. Quaglia, Receptor ligands as helping hands to L-DOPA in the treatment of parkinson's disease, *Biomolecules*, 2019, **9**, 142.

22 L. Lin, H. T. Lian, X. Y. Sun, Y. M. Yu and B. Liu, An l-dopa electrochemical sensor based on a graphene doped mole-cularly imprinted chitosan film, *Anal. Methods*, 2015, **7**, 1387–1394.

23 K. A. Kempadoo, E. V. Mosharov, S. J. Choi, D. Sulzer and E. R. Kandel, Dopamine release from the locus coeruleus to the dorsal hippocampus promotes spatial learning and memory, *Proc. Natl. Acad. Sci. U. S. A.*, 2016, **113**, 14835–14840.

24 P. C. Rodriguez, D. B. Pereira, A. Borgkvist, M. Y. Wong, C. Barnard, M. S. Sonders, H. Zhang, D. Sames and D. Sulzer, Fluorescent dopamine tracer resolves individual dopaminergic synapses and their activity in the brain, *Proc. Natl. Acad. Sci. U. S. A.*, 2013, **110**, 870–875.

25 X. Yan, D. Pan, H. Wang, X. Bo and L. Guo, Electrochemical determination of L-dopa at cobalt hexacya-noferrate/large- mesopore carbon composite modified elec-trode, *J. Electroanal. Chem.*, 2011, **663**, 36–42.

26 F. Elbarbry, V. Nguyen, A. Mirka, H. Zwickey and R. Rosenbaum, A new validated HPLC method for the determination of levodopa: Application to study the impact of ketogenic diet on the pharmacokinetics of levodopa in Parkinson's participants, *Biomed. Chromatogr.*, 2019, **33**, 1–7.

27 S. W. Park, T. E. Kim and Y. K. Jung, Glutathione-decorated fluorescent carbon quantum dots for sensitive and selective detection of levodopa, *Anal. Chim. Acta*, 2021, **1165**, 338513.

28 K. J. Goswami, A. Boruah and N. S. Sarma, Smart-phone-assisted optical biosensors based on silk-fibroin-decorated reduced graphene oxide quantum dots for fluorescent turn-on recognition of L-dopa, *ACS Appl. Nano Mater.*, 2023, **6**, 10191–10201.

29 F. Zhu, J. Wang, S. Xie, Y. Zhu, L. Wang, J. Xu, S. Liao, J. Ren, Q. Liu, H. Yang and X. Chen, l -Pyroglutamic acid-modified CdSe/ZnS quantum dots: A new fluorescence-responsive chiral sensing platform for stereospecific mole-cular recognition, *Anal. Chem.*, 2020, **92**, 12040–12048.

30 H. P. Wu, T. L. Cheng and W. L. Tseng, Phosphate-modi-fied TiO_2 nanoparticles for selective detection of dopa-mine, levodopa, adrenaline, and catechol based on fluo-rescence quenching, *Langmuir*, 2007, **23**, 7880–7885.

31 J. Dong, X. Li, S. B. Peh, Y. Di Yuan, Y. Wang, D. Ji, S. Peng, G. Liu, S. Ying, D. Yuan, J. Jiang, S. Ramakrishna and D. Zhao, Restriction of molecular rotors in ultrathin two-dimensional covalent organic framework nanosheets for sensing signal amplification, *Chem. Mater.*, 2019, **31**, 146–160.

32 B. Si and E. Song, Recent advances in the detection of neu-rotransmitters, *Chemosensors*, 2018, **6**, 1–24.

33 R. Baron, M. Zayats and I. Willner, Dopamine-, L-DOPA-, adrenaline-, and noradrenaline-induced growth of Au nanoparticles: Assays for the detection of neurotransmit-ters and of tyrosinase activity, *Anal. Chem.*, 2005, **77**, 1566–1571.

34 J. Soleymani, Advanced materials for optical sensing and biosensing of neurotransmitters, *TrAC, Trends Anal. Chem.*, 2015, **72**, 27–44.

35 K. E. Secor and T. E. Glass, Selective amine recognition: Development of a chemosensor for dopamine and norepi-nephrine, *Org. Lett.*, 2004, **6**, 3727–3730.

36 H. Yan, Y. Wang, F. Huo and C. Yin, Fast-specific fluo-rescent probes to visualize norepinephrine signaling path-ways and its flux in the epileptic mice brain, *J. Am. Chem. Soc.*, 2023, **145**, 3229–3237.

37 Y. Mei, Q. W. Zhang, Q. Gu, Z. Liu, X. He and Y. Tian, Pillar [5]arene-based fluorescent sensor array for biosensing of intracellular multi-neurotransmitters through host–guest recognitions, *J. Am. Chem. Soc.*, 2022, **144**, 2351–2359.

38 T. Imada, H. Kijima, M. Takeuchi and S. Shinkai, Selective binding of glucose-6-phosphate, 3,4-dihydroxyphenylalanine (DOPA) and their analogs with a boronic-acid-appended metalloporphyrin, *Tetrahedron*, 1996, **52**, 2817–2826.

39 A. Coskun and E. U. Akkaya, Three-point recognition and selective fluorescence sensing of ʟ-DOPA, *Org. Lett.*, 2004, **6**, 3107–3109.

40 Z. Wu, X. Yang, W. Xu, B. Wang and F. Hao, A new boronic acid-based fluorescent sensor for ʟ-dihydroxy-phenylalanine, *Drug Discoveries Ther.*, 2011, **6**, 238–241.

41 G. F. Whyte, R. Vilar and R. Woscholski, Molecular recognition with boronic acids—applications in chemical biology, *J. Chem. Biol.*, 2013, **6**, 161–174.

42 E. J. Jun, H. Liub, J. Y. Choi, J. Y. Lee and J. Yoon, New fluorescent receptor composed of two imidazoliums, two pyrenes and a boronic acid for the recognition of DOPAC, *Sens. Actuators, B*, 2013, **176**, 611–617.

43 I. J. Bazany-Rodríguez, M. K. Salomón-Flores, A. O. Viviano-Posadas, M. A. García-Eleno, D. Martínez-Oteroc and A. Dorazco-González, Chemosensing of neurotransmitters with selectivity and naked eye detection of L-DOPA based on fluorescent Zn(ɪɪ)-terpyridine bearing boronic acid complexes, *Dalton Trans.*, 2021, **50**, 4255–4269.

44 M. K. Salomón-Flores, J. Valdes-García, A. O. Viviano-Posadas, D. Martínez-Otero, J. Barroso-Flores, I. J. Bazany-Rodríguez and A. Dorazco-González, Molecular two-point recognition of fructosyl valine and fructosyl glycyl histidine in water by fluorescent Zn(ɪɪ)-terpyridine complexes bearing boronic acids, *Dalton Trans.*, 2024, **53**, 8692–8708.

45 K. M. T. John and W. Bunting, Stability constants for some 1:1 metal-carboxylate complexes, *Can. J. Chem.*, 1970, **48**, 1650–1656.

46 T. Hashemzadeh, M. A. Haghighatbin, J. Agugiaro, D. J. D. Wilson, C. F. Hogan and P. J. Barnard, Luminescent iridium(ɪɪɪ)–boronic acid complexes for carbohydrate sensing, *Dalton Trans.*, 2020, **49**, 11361–11374.

47 A. O. Viviano-Posadas, U. Romero-Mendoza, I. J. Bazany-Rodríguez, R. V. Velázquez-Castillo, D. Martínez-Otero, J. M. Bautista-Renedo, N. González-Rivas, R. Galindo-Murillo, M. K. Salomón-Flores and A. Dorazco-González, Efficient fluorescent recognition of ATP/GTP by a water-soluble bisquinolinium pyridine-2,6-dicarboxamide compound. Crystal structures, spectroscopic studies and interaction mode with DNA, *RSC Adv.*, 2022, **12**, 27826–27838.

48 I. J. Bazany-Rodríguez, D. Martínez-Otero, J. Barroso-Flores, A. K. Yatsimirsky and A. Dorazco-González, Sensitive water-soluble fluorescent chemosensor for chloride based on a bisquinolinium pyridine–dicarboxamide compound, *Sens. Actuators, B*, 2015, **221**, 1348–1355.

49 S. Martínez-Vargas, A. Dorazco-González, S. Hernández-Ortega, R. A. Toscano, J. E. Barquera-Lozada and J. Valdés-

Martínez, Interaction between aromatic rings as organizing tools and semi-coordination in Cu(ɪɪ) compounds, *CrystEngComm*, 2017, **19**, 4595–4604.

50 R. Khattar and P. Mathur, 1-(Pyridin-2-ylmethyl)-2-(3-(1-(pyridin-2-ylmethyl)benzimidazol-2-yl) propyl) benzimidazole and its copper(ɪɪ) complex as a new fluorescent sensor for dopamine (4-(2-aminoethyl)benzene-1,2-diol), *Inorg. Chem. Commun.*, 2013, **31**, 37–43.

51 A. K. Purohit, S. K. Padhan, J. R. Mohanty and P. K. Kar, Chromo-luminescent selective detection of fluoride ions by a copper(ɪɪ) bis(terpyridine) complex solution via a displacement approach, *Photochem. Photobiol. Sci.*, 2018, **17**, 815–821.

52 R. Badugu, J. R. Lakowicz and C. D. Geddes, Fluorescence sensors for monosaccharides based on the 6-methylquinolinium nucleus and boronic acid moiety: Potential application to ophthalmic diagnostics, *Talanta*, 2005, **65**, 762–768.

53 J. A. Peters, Interactions between boric acid derivatives and saccharides in aqueous media: Structures and stabilities of resulting esters, *Coord. Chem. Rev.*, 2014, **268**, 1–22.

54 G. Springsteen and B. Wang, A detailed examination of boronic acid-diol complexation, *Tetrahedron*, 2002, **58**, 5291–5300.

55 Y. Suzuki, D. Kusuyama, T. Sugaya, S. Iwatsuki, M. Inamo, H. D. Takagi and K. Ishihara, Reactivity of boronic acids toward catechols in aqueous solution, *J. Org. Chem.*, 2020, **85**, 5255–5264.

56 W. L. A. Brooks, C. C. Deng and B. S. Sumerlin, Structure–reactivity relationships in boronic acid–diol complexation, *ACS Omega*, 2018, **3**, 17863–17870.

57 T. D. James, K. R. A. S. Sandanayake and S. Shinkai, A glucose-selective molecular fluorescent sensor, *Angew. Chem., Int. Ed. Engl.*, 1994, **33**, 2207–2209.

58 J. Valdes-García, J. Zamora-Moreno, M. K. Salomón-Flores, D. Martínez-Otero, J. Barroso-Flores, A. K. Yatsimirsky, I. J. Bazany-Rodríguez and A. Dorazco-González, Fluorescence sensing of monosaccharides by bis-boronic acids derived from quinolinium dicarboxamides: structural and spectroscopic studies, *J. Org. Chem.*, 2023, **88**, 2174–2189.

59 R. Badugu, J. R. Lakowicz and C. D. Geddes, Boronic acid fluorescent sensors for monosaccharide signaling based on the 6-methoxyquinolinium heterocyclic nucleus: Progress toward noninvasive and continuous glucose monitoring, *Bioorg. Med. Chem.*, 2005, **13**, 113–119.

60 R. Badugu, J. R. Lakowicz and C. D. Geddes, A wavelength-ratiometric fluoride-sensitive probe based on the quinolinium nucleus and boronic acid moiety, *Sens. Actuators, B*, 2005, **104**, 103–110.

61 R. Badugu, J. R. Lakowicz and C. D. Geddes, Excitation and emission wavelength ratiometric cyanide-sensitive probes for physiological sensing, *Anal. Biochem.*, 2004, **327**, 82–90.

62 M. Regueiro-Figueroa, K. Djanashvili, D. Esteban-Gómez, T. Chauvin, É. Tóth, A. De Blas, T. Rodríguez-Blas and C. Platas-Iglesias, Molecular recognition of sialic acid by

lanthanide(III) complexes through cooperative two-site binding, *Inorg. Chem.*, 2010, **49**, 4212–4223.

63 T. Tanaka, Y. Nishiura, R. Araki, T. Saido, R. Abe and S. Aoki, ^{11}B NMR probes of copper(II): Finding and implications of the Cu^{2+}-promoted decomposition of *ortho*-carborane derivatives, *Eur. J. Inorg. Chem.*, 2016, 1819–1834.

64 S. Gamsey, N. A. Baxter, Z. Sharrett, D. B. Cordes, M. M. Olmstead, R. A. Wessling and B. Singaram, The effect of boronic acid-positioning in an optical glucose-sensing ensemble, *Tetrahedron*, 2006, **62**, 6321–6331.

65 S. A. Valenzuela, J. R. Howard, H. M. Park, S. Darbha and E. V. Anslyn, ^{11}B NMR spectroscopy: Structural analysis of the acidity and reactivity of phenyl boronic acid–diol condensations, *J. Org. Chem.*, 2022, **87**, 15071–15076.

66 A. Dorazco-González and A. K. Yatsimirsky, Binding of ureas and amides to a Cu(II) terpyridine complex in methanol, *Inorg. Chim. Acta*, 2010, **363**, 270–274.

67 G. Fang, H. Wang, Z. Bian, J. Sun, A. Liu, H. Fang, B. Liu, Q. Yao and Z. Wu, Recent development of boronic acid-based fluorescent sensors, *RSC Adv.*, 2018, **8**, 29400–29427.

68 S. D. Bull, M. G. Davidson, J. M. H. van den Elsen, J. S. Fossey, A. T. A. Jenkins, Y. Jiang, Y. Kubo, F. Marken, K. Sakurai, J. Zhao and T. D. James, Exploiting the reversible covalent bonding of boronic acids: Recognition, sensing, and assembly, *Acc. Chem. Res.*, 2013, **46**, 312–326.

69 V. Amendola, G. Bergamaschi, A. Buttafava, L. Fabbrizzi and E. Monzani, Recognition and sensing of nucleoside monophosphates by a dicopper(II) cryptate, *J. Am. Chem. Soc.*, 2010, **132**, 147–156.

70 R. V. Velázquez-Castillo, M. K. Salomón-Flores, A. O. Viviano-Posadas, I. J. Bazany-Rodríguez, C. Bustos-Brito, J. M. Bautista-Renedo, N. González-Rivas, L. D. Rosales-Vázquez and A. Dorazco-González, Recognition and visual detection of ADP and ATP based on a dinuclear Zn(II)-complex with pyrocatechol violet in water, *Dyes Pigm.*, 2021, **196**, 109827.

71 C. Schmuck and M. Schwegmann, A naked-eye sensing ensemble for the selective detection of citrate —but not tartrate or malate—in water based on a tris-cationic receptor., *Org. Biomol. Chem.*, 2006, **4**, 836–838.

72 M. J. Frisch, G. W. Trucks, H. B. Schlegel, G. E. Scuseria, M. A. Robb, J. R. Cheeseman, G. Scalmani, V. Barone, G. A. Petersson, H. Nakatsuji, X. Li, M. Caricato, A. V. Marenich, J. Ioino, B. G. Janesko, R. Gomperts, B. Mennucci, H. P. Hratchian, J. V. Ortiz, A. F. Izmaylov, J. L. Sonnenberg, D. Williams-Young, F. Ding, F. Lipparini, F. Egidi, J. Goings, B. Peng, A. Petrone, T. Henderson, D. Ranasinghe, V. G. Zakrzewski, J. Gao, N. Rega, G. Zheng, W. Liang, M. Hada, M. Ehara, K. Toyota, R. Fukuda, J. Hasegawa, M. Ishida, T. Nakajima, Y. Honda, O. Kitao, H. Nakai, T. Vreven, K. Throssell, J. A. Montgomery Jr., J. E. Peralta, F. Ogliaro, M. J. Bearpark, J. J. Heyd, E. N. Brothers, K. N. Kudin, V. N. Staroverov, T. A. Keith, R. Kobayashi, J. Normand, K. Raghavachari, A. P. Rendell, J. C. Burant, S. S. Iyengar, J. Tomasi, M. Cossi, J. M. Millam, M. Klene, C. Adamo, R. Cammi, J. W. Ochterski, R. L. Martin, K. Morokuma, O. Farkas, J. B. Foresman and D. J. Fox, *Gauss View 5.0*, Gaussian, Inc., Wallingford, USA, 2016.

73 *Bruker SAINT and SADABS*, Bruker AXS Inc., Madison, Wisconsin, USA, 2007.

74 G. M. Sheldrick, A short history of SHELX, *Acta Crystallogr., Sect. A: Found. Crystallogr.*, 2007, **64**, 112–122.

75 C. B. Hübschle, G. M. Sheldrick and B. Dittrich, ShelXle: A Qt graphical user interface for SHELXL, *J. Appl. Crystallogr.*, 2011, **44**, 1281–1284.

76 Persistence of Vision Raytracer (version 3.6), Persistence of Vision Raytracer (Version 3.6), **https://www.povray.org**.

77 GIMP 2.8: The GNU Image Manipulation Program, **https://www.gimp.org**, *GIMP 2.8 GNU Image Manip. Program*, **http//www.gimp.org**.